# Mixed-state thermoelectric and thermomagnetic effects of a $Bi_2Sr_2CaCu_2O_{8+\delta}$ single crystal

M. Pęka
*Department of Chemistry, University of Warsaw, Al. Zwirki i Wigury 101, PL-02-089 Warsaw, Poland and SUPRAS, Institut d'Electricite Montefiore, University of Liege, B28, Sart Tilman, B-4000 Liege, Belgium*

E. Mąka
*Department of Chemistry, University of Warsaw, Al. Zwirki i Wigury 101, PL-02-089 Warsaw, Poland*

D. Hu and V. Brabers
*Department of Physics, Eindhoven University of Technology, 5600 MB Eindhoven, The Netherlands*

M. Ausloos*
*Institute of Physics, SUPRAS,† University of Liege, B5, Sart Tilman, B-4000 Liege, Belgium*
(Received 25 January 1995; revised manuscript received 25 April 1995)

We examined the electric and thermoelectric transport properties of a superconducting $Bi_2Sr_2CaCu_2O_{8+\delta}$ single crystal. The magnetic fields lower than 4 T were applied perpendicular to the electrical or thermal gradient along the $c$ axis. All properties are described in terms of temperature-integrated excess quantities as a function of the magnetic field. Power-law exponents are compared to those found on other two-dimensional (2D) and 3D polycrystalline or textured systems. The apparent dimensionality of the system is emphasized. The values of various derived quantities are also given and compared to those of other high-temperature superconductors. These quantities are the vortex transport entropy (ca. $10^{-15}$ J/K m), the viscous damping coefficient ($1.2\times10^{-9}$ J s/m$^3$ at 78 K), the Ginzburg-Landau parameter (between 70 and 120), the thermal Hall angle, and the activation energies for each transport property. The findings point out the need of including the system dimensionality and various vortex pinning and vortex scattering effects in theoretical calculations.

## I. INTRODUCTION

It is of fundamental interest to study a high-temperature superconductor's (HTSC) response to magnetic fields.[1] An interesting class of materials is that of anisotropic Bi-based $22(n-1)n$ structures. Among the most interesting properties are those resulting from transport phenomena. Such thermomagnetic transport properties have, of course, already received some attention.[2–8] However, to our knowledge there are not many papers dealing with the Nernst effect and the characteristic parameters of the mixed state in the $Bi_2Sr_2CaCu_2O_{8+\delta}$ (BSCCO) systems. Apparently the most exhaustive investigation of electrical, related Hall, and Nernst properties is due to Dascoulidou *et al.*[2] However, this ground breaking paper dealt with a granular BSCCO, not specifically single phase. Some of us have also collaborated in work on polycrystalline Bi2223 (Refs. 9 and 10) and textured Bi2223 (Ref. 11) HTSC.

Theoretical papers like that of Samoilov and coworkers[3–5] also pertain to the present work. The fundamental aspect of these investigations reside in understanding and/or deducing properties of the so-called mixed state of HTSC materials. The best procedure is to investigate such properties in single-crystal materials, since in this form the microstructure is then well defined. The case of films[8] and textured systems[12] also needs some attention for completeness.

We have grown a single crystal of Bi2212 and have endeavored to specifically measure its Nernst effect. This effect is produced by applying a magnetic field perpendicular to a thermal gradient established in a conductor. Like the Hall effect, it is a transverse one[13] and is characterized by the Nernst coefficient defined by

$$N=\frac{E_y}{B_z\nabla T_x}\ , \tag{1}$$

where $B_z$ is the magnetic-flux density, $E_y$ is the observed transverse electric field, and $\nabla T_x$ is the applied temperature gradient. An elementary kinetic theory[13] leads to the observation that the Nernst coefficient is independent of the charge carrier, and should be of the opposite sign to the variation of the scattering rate of carriers with energy measured at the Fermi level. The Nernst coefficient should thus be positive (negative) if the relaxation time is a monotonically decreasing (increasing) function of energy. In normal metals, its signs and variations are not yet understood. In the mixed state, it is thought that the Nernst coefficient is dominated by the transport of magnetic-flux lines. To study the Nernst effect thus would lead to more information on the nature of the mixed state, and maybe could allow one to decide between various models, like the vortex glass[14] or liquid state(s),[15] and the effect of thermal depinning,[16] vortex lattice melting,[15,17] and flux creep.[18–20] For completeness, we also present the electrical resistivity and thermoelectric power. All properties were measured in the presence of magnetic fields lower than 4 T.

 

In Sec. II, we describe the sample preparation and characterization, while in Sec. III we briefly describe the experimental setups and runs. In Sec. IV A and IV B, we shortly present the data on the electrical resistivity and thermoelectric power. The Nernst effect is found in Sec. IV C. The data analysis is made in Sec. V for all these properties. In particular, we discuss the mixed-state resistivity and the corresponding percolation line in Sec. V A. Section V B contains the analysis of the mixed-state thermoelectric power. We discuss the Nernst effect and also derive and comment about the transport entropy (Sec. V C), the Ginzburg-Landau parameter (Sec. V D), the Hall angle (Sec. V E), and the activation energies (Sec. V F).

## II. SAMPLES

Single crystals of $Bi_2Sr_2CaCu_2O_{8-z}$ were grown by the traveling solvent floating-zone method (TSFZ). Powders of $Bi_2O_3$, $CaCO_3$, $SrCO_3$, and CuO in stoichiometric ratio were mixed and sintered twice at 860°C in flowing oxygen for 24 h with intermediate grinding. The obtained powders were filled into 8 mm diameter wide rubber tubes isostatically pressed at 3 kbar. The bars were sintered again at 865°C in flowing air for 24 h.

For the TSFZ method a homebuilt optical radiation furnace was used with a 2.5 kW xenon lamp as the radiation source. The radiation from the lamp was focused on the polycrystalline bars by means of two elliptical mirrors, forming a molten zone. A high pulling rate of 80 mm/h was first used for improving the density of the bars, whence preventing the soaking of the melt into the porous bars. After that the densified bars were zone melted with a pulling rate of 1 mm/h under an atmosphere of 2 bars flowing air. The rotation rate of the bars was about 40 cycles/min.

Large single crystals with typical $10\times3\times0.3$ mm$^3$ dimensions could be separated from the obtained bars. The single crystalline nature of the most useful sample was confirmed by x-ray diffraction and Laue transmission photographs. One sample was thoroughly investigated. Other grown single crystals were characterized by energy dispersive x-ray analysis and scanning electron microscopy. Several tests were made through coefficients such as electrical resistivity in order to check the critical temperature and the transition width. The data were as reproducible as can be expected for such kinds of materials. However, for measurements implying thermal gradients a "not too small size sample" is necessary to make the heater contact and create a proper temperature gradient. Therefore only the largest available single crystal was used for measuring thermoelectric and thermomagnetic effects. Without definite experimental proof, we expect, however, that the data well reproduces the characteristics of the investigated effects for these HTSC materials. It is known that a few percent quantitative spread is possible in such materials.

The single crystals grown without twinning have $c=30.97$ Å and $a\cong b=5.4$ Å lattice parameters, respectively. The superlattice along the $b$ axis with a periodicity of $4.7b$ was observed. However, since the accuracy of the present resistivity or thermomagnetic measurements do not distinguish between the $a$ and $b$ axis, this problem was not studied in detail. The $c$ axis in the measured sample was perpendicular to the greatest sample surface. Wet chemical analysis gave the composition of the single crystals very close to the nominal one. No evidence of the Bi2223 phase was found within the accuracy of the x-ray, ac resistivity, and resistivity measurements. For more details of preparation and characterization see Ref. 21.

## III. MEASUREMENTS

The magnetotransport properties could be effectively measured only for the magnetic field applied along the $c$ axis. Due to the sample geometry the transport measurements were made in the $ab$ plane applying the external magnetic field along the shortest $c$ axis. All measurements were performed inside a closed-cycle refrigerator CTI M22 filled with the helium exchange gas. The temperature of the sample holder was stabilized with 50 mK accuracy and measured using a CGR thermometer and a Lake Shore DRC-91CA temperature controller. The magnetic field was supplied by a Magnex Scientific superconducting magnet. Electrical resistivity was measured by means of the four-probe method with dc current reversing several times in order to eliminate influence of spurious voltages. The differential thermoelectric power and Nernst effect were measured with one end of the sample kept in good thermal contact with a heat sink. The temperature gradient was stabilized between 10 and 15 K/cm by a small heater located at the opposite end of the sample. The dc heater supplied a power of 5–50 mW. The temperature of the sample was measured by two copper-constantan thermocouples placed in good thermal contact with the sample. Two pairs of high-purity copper leads were electrically connected to the sample either parallel or perpendicular to the temperature gradient to measure the Seebeck and Nernst voltages, respectively. Voltages were measured using a Keithley 705 scanner and Keithley 182 nanovoltmeter with 30 nV accuracy. The thermoelectric power of the copper leads was subtracted. Measurements started when the sample was in the normal state above 160 K and finished near a temperature between 20 and 30 K. The temperature variation was in small steps between 0.25 and 1 K. A delay time of 30–100 s was used before each measurement recording in order to achieve a thermal steady state. The magnetic field was varied from low to high values. Details of the measuring techniques were basically the same as described previously.[9–12]

## IV. RESULTS

### A. Electrical resistivity

The electrical resistivity at 100 K is of the order of 5 $\mu\Omega$ m and is comparable with values of 0.3, 0.8, and 3 $\mu\Omega$ m reported by Refs. 22, 23, and 24, respectively. The normal-state resistivity rises proportionally to temperature at the mean rate of $2\times10^{-8}$ $\Omega$/K as for "metallic-like" HTSC. Deviations from the linear temperature

variation of resistivity start to appear below 105 K. The most abrupt resistivity drop occurs between 95 and 85 K in absence of magnetic field (Fig. 1). The critical temperature $T_c$ for which the coherence length of the intragrain superconductivity fluctuations diverges is usually close to the midpoint transition and is found to be 92 K here. The percolation temperature $T_p$ at which the first superconducting path occurs in the system due to the wave-function phase-coherence perfect matching between superconducting grains is equal to 70 K. A comparison of this resistivity variation with the data reported by Van Driessche, Cattoir, and Hoste[25] allows us to conclude that the oxygen nonstoichiometry of the superconductors $Bi_2Sr_2CaCu_2O_{8+\delta}$ may be estimated to be $\delta \cong 0.18$.

The application of an external magnetic field along the $c$ axis gradually broadens the transition interval. For each applied field strength the transition markedly starts at about 95 K but the resistivity decay becomes less abrupt for higher magnetic fields, as indicated in Fig. 1. In fact the transition is complete around 45 K at $H=4$ T. No magnetoresistivity was observed in the normal state in magnetic fields between 1 and 4 T. One should note that the $R(T)$ decay occurs without knee for any magnetic field.

### B. Thermoelectric power

The thermoelectric power (TEP) behavior (Fig. 2) is typical of the bismuth-based HTSC (Refs. 26–30) consisting of a roughly linear decrease in the normal state with a smeared TEP maximum (7 $\mu$V/K) just above the transition temperature.[31] The mean rate of TEP variation in the normal state is about $-6\times10^{-8}$ V/K$^2$. From a two-dimensional (2D) theory of TEP one can obtain that the Fermi energy is equal to 1.2 eV.[32,33] The TEP drop is most abrupt for zero magnetic field, when TEP disappears at 75 K (Fig. 3), which can be considered a percolation temperature as well. It has been pointed out that for the vanishing TEP the fraction of superconducting material can be smaller than for the vanishing resistance.[34] For higher magnetic fields the transition gradually spreads out and for $H=4$ T, it is complete at 60 K.

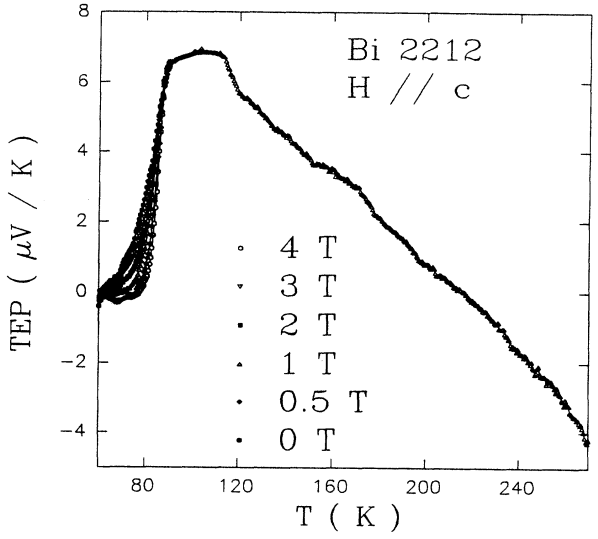


FIG. 2. Thermoelectric power vs temperature of a Bi2212 single crystal at various magnetic-field strengths.

It is of interest to comment on the normal-state behavior. It is usually thought that the sign of the TEP reflects the sign of the majority carriers.[35] This is far from the truth.[36,37] It can be shown that when taking elastic and inelastic scattering of electrons by acoustic phonons, the TEP behavior presents a minimum at low

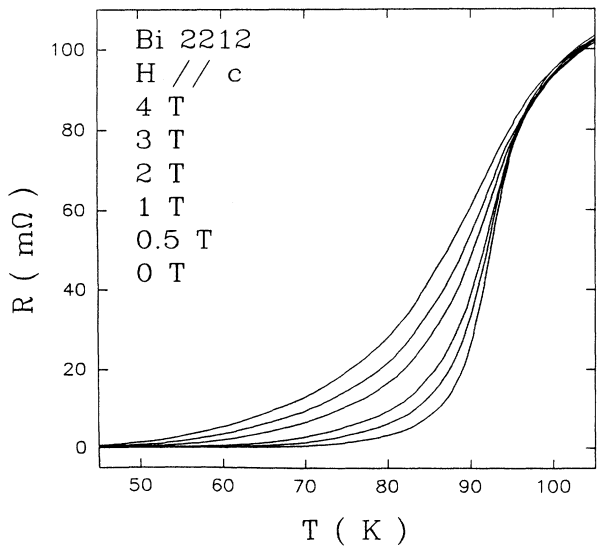


FIG. 1. Electrical resistance vs temperature of Bi2212 single crystal at various magnetic-field strengths.

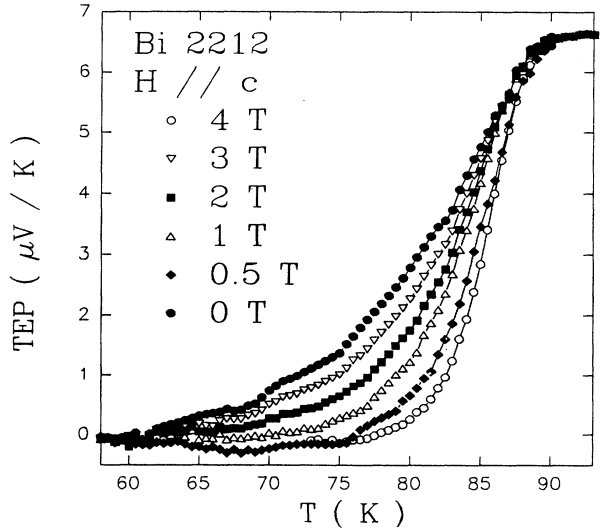


FIG. 3. Thermoelectric power vs temperature around the superconducting transition in Bi2212 single crystal at various magnetic-field strengths.

temperature followed by a maximum at intermediate temperature, and a negative slope thereafter;[38] the latter maximum being even positive. For two-band charge carriers with opposite signs the TEP behavior is still more complex.[36,37] Therefore the change in TEP sign near room temperature is not necessarily related to a change in sign of the carriers. The origin of the features at intermediate temperature can receive a simple interpretation consistent with the recalled "horizontal and scattering processes"[39] and the inherent distortion of the carrier density of states near the Fermi level in a temperature gradient. The observed bump in the normal-state TEP of an HTSC is in fact of the order of magnitude of that theoretically predicted.[36,37,40–42] Thus, the bump was often attributed to a phonon drag mechanism even though the temperature region might not be at all correct. It might be just a normal-state background specific to TEP, and irrelevant for superconducting properties. In this respect it can be noticed that the Hall effect on such materials is positive up to room temperature[5] even though the TEP changes sign.[43,44]

### C. Nernst effect

The Nernst effect (NE) in the normal state of Bi2212 single crystals is negative and weakly temperature dependent. This is similar to the behavior of the normal-state Nernst effect in Tl2212 thin films reported by Clayhold *et al.*[45] However, the NE exhibits much variation in the mixed state in such type-II superconductors (Fig. 4). In the vicinity of the transition temperature the Nernst effect appears to be positive at temperatures shifting from 91 to 88 K for a magnetic field rising from 0.5 to 4 T. At 0.5 T the Nernst signal occurs on a relatively narrow interval (about 7 K at half width) and attains a high value of 0.9 $\mu$V/K at 88 K. For 1 T the Nernst spectrum contains two peaks: a narrow peak centered at 88 K and the broad maximum at 64 K. The narrow peak is suppressed at large magnetic field. For $H=2$ T some trace of the weak peak at 88 K is followed by a broad maximum at 70 K. At higher magnetic field only a broad maximum up to 0.4 $\mu$V/K at 65 K is observed. The broad NE signal is only slightly lower than that reported by Zavaritsky, Samoilov, and Yurgens.[46]

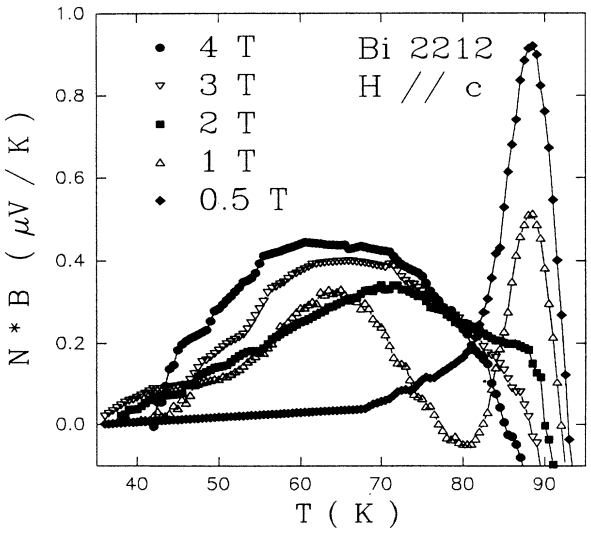


FIG. 4. Product of the Nernst coefficient $N$ by the magnetic field $B$ as a function of temperature for a Bi2212 single crystal registered during cooling at various magnetic fields.

To our knowledge such findings have not been reported for NE in HTSC. Several interpretations of the features can be presented. The first one can be found in a possible misorientation of the magnetic field, leading to a signal due to pancake vortex structures. This would, however, lead to a signal without split peaks, similar to that in a polycrystalline system. The same holds true if there are random internal weak links. In fact, these weak links are not seen in the temperature variation of electrical resistivity. Oxygen inhomogeneity could be another cause for NE peak structure. However, this would give a broad transition in $R(T)$ and $Q(T)$ instead of the sharp one observed at 75 K. Another possibility is a complex long-range internal modulation in the single crystal leading to an intragrain granularity effect. This *ad hoc* argument should be right if some hysteresis was found when going up and down with the temperature at smaller magnetic fields.[33] This could not be tested because the NE is then too small and the error bars are too large. The variation of NE with $T$ and $H$ reminds us indeed of the behavior of the imaginary part of the ac susceptibility with intra- and intergranular components. To follow the peak evolution, it would be interesting to look for the angle dependence of $H$ with respect to the $c$ axis when $H$ is displaced from the perpendicular direction to the layers. However, here as in thin films,[8] the sample geometry does not allow for appropriate probe and heater positions.

## V. DISCUSSION

### A. Mixed-state resistivity

The excess resistance $\Delta R(T,H)$ determined by

$$\Delta R(T,H)=R(T,H)-R(T,H=0) \tag{2}$$

is negligible in the normal state. A finite excess resistance $\Delta R(T,H)$ values starts to appear in the fluctuation interval of $\sim 10$ K above the superconducting transition (Fig. 5). However, an abrupt rise of $\Delta R$ occurs in a narrow temperature interval below 95 K. The $\Delta R$ signal vanishes between 65 and 45 K when the magnetic-field strength is between 0.5 and 4 T. The integrated area $A(H)$ below the $\Delta R$ vs $T$ curve enables us to determine the exponent of the $A(H)\simeq H^a$ relation. The $a$ exponent is equal to $0.96\pm0.03$ and higher than the $\frac{2}{3}$ value which would be obtained[47] if one follows Tinkham's theory[48] and found, e.g., for polycrystalline Bi2223 superconductors.[9] This clearly shows that the Tinkham exponent is dimensionality dependent. The discussion of the resistivity broadening in a field should take such dimensionality ingredients into account.

The electrical resistivity vs temperature variation extrapolated down to the mean noise level[49] allows us to

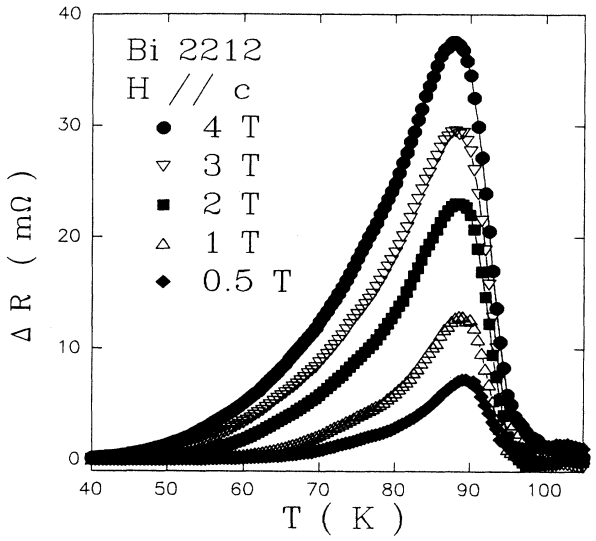


FIG. 5. Mixed-state excess resistance $\Delta R$ of a Bi2212 single crystal versus temperature at various magnetic-field strengths.

determine the so-called percolation line $H_R(T)$ shown in Fig. 6. In other words, the percolation line is hereby defined as the relationship between the percolation temperature at which the resistivity falls below measurable value and the magnetic field $H_R$ which is breaking the grain connectivity, hence inducing an intergrain resistance. It is worth noticing that this percolation line is located approximately 4–7 K above the so-called irreversibility line determined for the Bi2212 single crystals from the magnetization data by Hu *et al.*[50] Other relatively low so-called irreversibility lines were also found from susceptibility data for the Bi2212 single crystals by Ruyter *et al.*[51] In fact, the mixed-state electrical resistivity reflects the flux-flow region or vortex-antivortex fluctuation contribution[52] whereas the magnetic susceptibility and zero-field-cooled methods probe rather flux depinning phenomena.

The irreversibility line and hereby the percolation line can be modeled by

$$H(T)=H_0(1-T/T_c)^q \tag{3}$$

with the exponent equal to either $q=3/2$ for the giant flux-creep model,[53] $q=4/3$ for the vortex-glass model[54] or $q=2$ for the vortex lattice melting model.[55,56] The apparent linear law in Fig. 6 means that the exponent is close to 4/3 predicted for the vortex-glass model.[54,55] It might be argued that the 4/3 exponent is based on 3D arguments. It should be of interest to examine the vortex-glass model in strictly 2D regimes. The giant flux-creep model and vortex lattice melting model seem to be excluded here in order to interpret the above findings.

### B. Mixed-state thermoelectric power

The so-called mixed-state thermoelectric power $\Delta Q(T,H)$ defined by

$$\Delta Q(T,H)=Q(T,H)-Q(T,H=0) \tag{4}$$

appears only below 89 K and spreads gradually down to 60 K for magnetic field increasing from 0.5 to 4 T (Fig. 7). An even broader interval of $\Delta Q$ as large as 40 K was reported at $H\|c$ for Bi2212 single crystals by Zavaritsky, Samoilov, and Yurgens.[4] The area $B(H)$ below the $\Delta Q(T,H)$ vs $H$ curve may be fitted to a $B(H)\simeq H^b$ expression with $b=0.89\pm0.05$. This almost proportional dependence of $B$ vs $H$ is close to that one observed by Gridin *et al.*[57] for a polycrystalline Bi-based superconductor. The $b$ exponent equal to 1.34 and 1.09 was found for the polycrystalline and textured Bi2223 HTSC, respectively.[9]

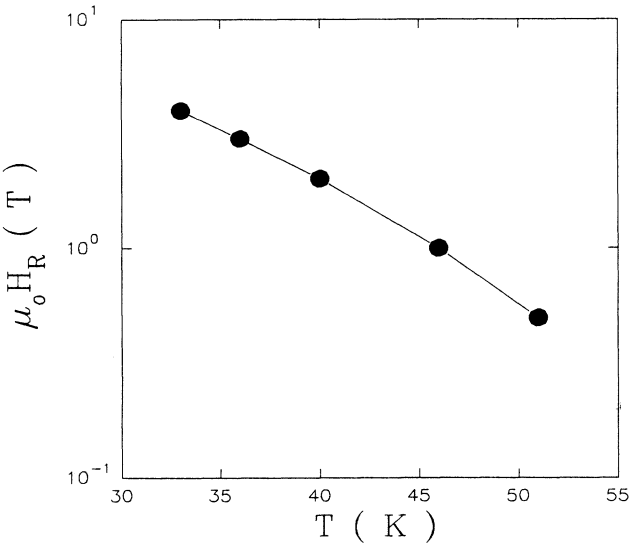


FIG. 6. The percolation line determined from electrical resistance.

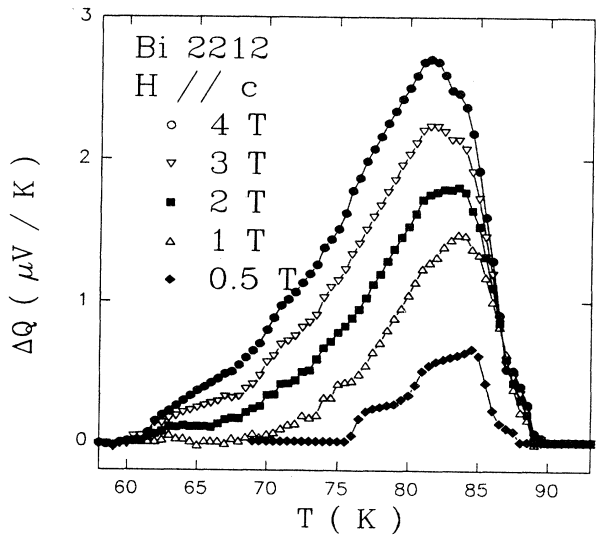


FIG. 7. Mixed-state thermoelectric power of a Bi2212 single crystal vs temperature at various magnetic-field strengths.

### C. Transport entropy

The transport entropy $S_\phi$ was calculated from the Nernst and mixed-state resistivity data as follows:

$$S_\phi = \phi_0 N^* B / \Delta\rho \ , \tag{5}$$

where $\phi_0$ is a flux quantum. $S_\phi$ appears abruptly below 93 K almost independently of the magnetic-field strength (Fig. 8). Only at the lowest fields like 0.5 and 1 T, does the $S_\phi$ vs $T$ plot reveal a maximum around 88 K. Values of $S_\phi$ increase when lowering the temperature below 80 K for any $H > 1$ T. The absolute values of $S_\phi$ are of the order $10^{-15}$ J/K m and fall in the range reported for polycrystalline[2,5] and textured (Refs. 9 and 11) Bi2223 HTSC. Taking into account that the thermal force $F_t$ acting on the unit length of the flux line[58] is related to transport entropy by

$$F_t = -S_\phi \nabla T \ , \tag{6}$$

one may estimate that $F_t$ reaches values up to $2\times10^{-12}$ N/m. This value is close to $F_t \cong 8\times10^{-13}$ N/m reported for Y123 thin films[8] and to $F_t \cong 10^{-13}$ N/m estimated for Bi2212 thin films from data given in Ref. 8.

The Nernst-effect data allowed us also to calculate the viscous damping coefficient of the vortex motion $\eta$ from the relation[59,60]

$$\eta = \phi_0 B / \Delta\rho \ . \tag{7}$$

From the mixed-state resistivity maximum at 88 K (Fig. 5) the local minimum of $\eta$ is equal to $1.2\times10^{-9}$ J s/m$^3$ at 78 K. Unfortunately, this $\eta$ parameter describing the response of the vortex system to the thermal driving force could not be compared with analog values for other HTSC due to the lack of such data known to the authors.

Within the time-dependent Ginzburg-Landau theory the transport entropy may be expressed as follows:

$$S_\phi = \frac{\phi_0 L_D(T)}{4\pi T} \frac{H_{c2}(T) - H}{1.16(2k_{GL}^2 - 1) + 1} \ , \tag{8}$$

where $k_{GL}$ is the Ginzburg-Landau parameter and $L_D(T)$ is a function approximately equal to 1 near $T_c$. The critical temperatures $T_c$ determined from the high-temperature part of the $S_\phi$ vs $T$ plots in Fig. 8, are simply related to the critical magnetic fields $H_{c2}$ as shown in Fig. 9. The slope of the $\mu_0 dH_{c2}/dT$ variation is equal to $-0.51$ T/K and is comparable to the $-0.36$ to $-0.39$ T/K values found for Bi2212 HTSC.[61,62] Somewhat higher values of $\mu_0 dH_{c2}/dT$ between $-0.9$ and $-1.36$ and $-1$ T/K were reported for the textured[11] and polycrystalline[2] Bi2223 HTSC, respectively. The $\mu_0 dH_{c2}/dT$ value obtained for Bi2212 thin films is equal to $-2.5$ T/K.[8]

Despite the relative scarcity of data the entropy exhibits a very specific dependence on the magnetic field (Fig. 10). At magnetic fields equal to or higher than 2 T the magnitude of the transport entropy diminishes gradually when the temperature rises from 65 to 90 K as shown in Fig. 10. Magnetic-field sensitive $S_\phi$ vs $H$ variation is observed at lower magnetic fields. At temperatures between 75 and 90 K the slope of the $S_\phi$ vs $H$ rises up at low magnetic fields. The $S_\phi$ maximum at $H = 1$ T shown in Fig. 10 for temperatures below 75 K becomes even higher and sharper at lower temperatures (not shown). Such as $S_\phi$ vs $H$ behavior is consistent with the theoretical models[63–65] predicting a $S_\phi$ maximum roughly at $T_c/2$. The low-field data of Fig. 10 suggest that the $S_\phi$ maximum occurs at weak magnetic fields when the temperature rises up to 90 K.

### D. Ginzburg-Landau parameter and penetration depth

A simple transformation of Eq. (8) supplies the Ginzburg-Landau parameter $k_{GL}$ as follows,

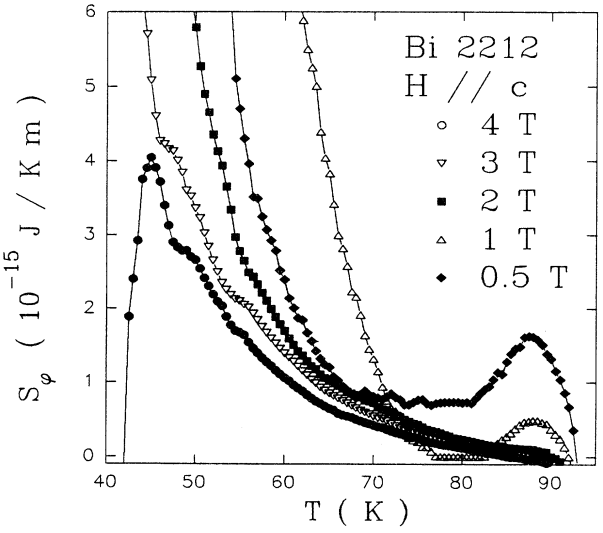


FIG. 8. Transport entropy as a function of temperature for a Bi2212 single crystal at various magnetic fields.

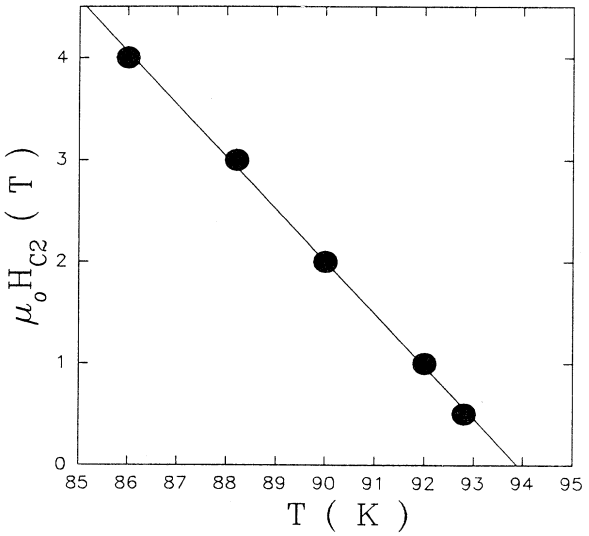


FIG. 9. The upper critical field $H_{c2}$ vs temperature determined from the transport energy.

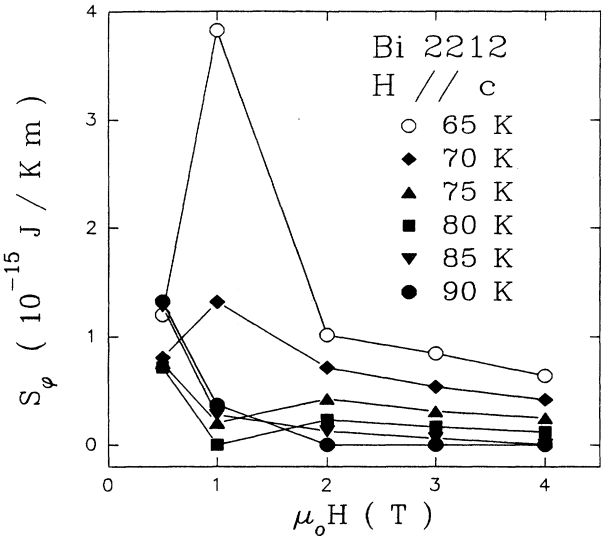


FIG. 10. Transport entropy vs magnetic field at various temperatures.

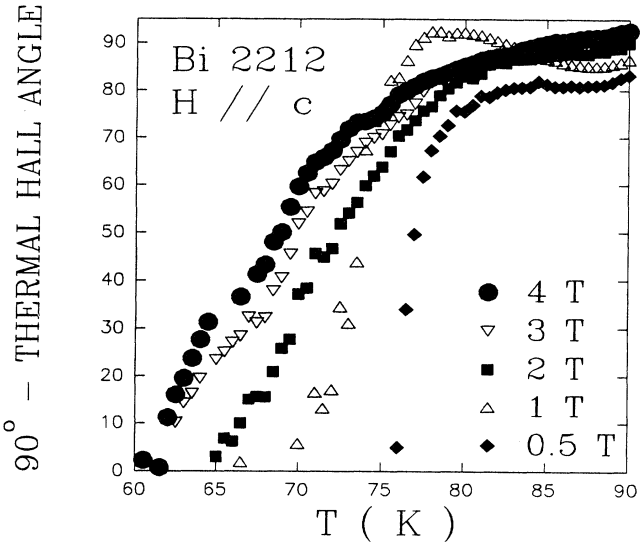


FIG. 11. Values of 90° thermal Hall angle vs temperature for various magnetic-field stengths.

$$k_{\mathrm{GL}}^2 \cong \frac{\phi_0}{13.28\pi T}\frac{dH_{c2}}{dT}\Big/\frac{dS_\phi}{dT} . \tag{9}$$

Values of $dS_\phi/dT$ determined from approximately linear $S_\phi$ vs $T$ variation just below $T_c$, range between $1.4\times10^{-17}$ and $4.7\times10^{-17}$ J/K$^2$ m. Furthermore, taking into account a linear relation between $H_{c2}(T)$ and $T$, as shown in Fig. 9, we arrive at $k_{\mathrm{GL}}$ values between 70 and 120. This range is close to the $k_{\mathrm{GL}}$ value $\cong 65\pm10$ derived from transport measurements at the $H\|c$ configuration in textured Bi2223 HTSC.[11] Such values are in agreement with $k_{\mathrm{GL}}=62.7$, as determined from magnetization in polycrystalline (Bi,Pb)2223 HTSC.[66]

In the next step assuming the London penetration depth $\lambda\cong10$ to 50 nm (Refs. 67 and 68), the coherence length $\xi_c$ may be estimated to be between 0.1 and 0.7 nm. It is remarkable that such a low $\xi_c$ value is shorter than the layer spacing as often observed in HTSC indeed.

### E. Thermal Hall angle

The thermal Hall angle $\alpha_t$ determined from the electric fields arising in the mixed state is defined by

$$\alpha_t=\arctan(N^*B/Q) . \tag{10}$$

It reveals the direction of the vortex velocity when the vortex is subjected to crossed thermal and magnetic forces. The data of Fig. 11 show that the vortices move at a mean $\alpha_t$ angle rising up to 90° with the temperature gradient as the temperature is lowered. The maximal value is attained around 75 K for $H=0.5$ T and shifts gradually to approximately 60 K at 4 T. Such high values of $\alpha_t$ seem to be typical for the Bi-based HTSC.[69,70] We may conclude from these data that at lower temperature vortices become pinned, whence leading to the vanishing of the Nernst electric field perpendicular to the temperature gradient. On the other hand the Seebeck electric field along the temperature gradient does not decay so abruptly. This points out the fact that vortex dissipation is not responsible for the thermoelectric effect in the mixed state of HTSC. It should be emphasized that such properties have not only a staticlike ("entropy") contribution but also should be calculated taking into account the scattering processes of quasiparticles on one hand, and nonequilibrium distribution functions of scatterers (vortex drag) on the other hand. From that point of view one should recall that there are two types of vortices which can scatter electrons: bound vortices and free ones. The latter ones, beside implying dissipation, do also lead to a static electric field.

### F. Activation energy

Assuming that thermally activated processes in the mixed state can be averaged and described by an Arrhenius law, an activation energy $U_G$ was determined as

$$U_G=d(\ln G)/d(1/H) , \tag{11}$$

where $G$ stands for either resistivity, Seebeck or Nernst coefficient, respectively. The zero magnetic-field values of $U$ are equal to 86 and 268 meV when determined from the resistivity and TEP, respectively. The $U_R$ and $U_Q$ values diminish at high magnetic fields as shown in Fig. 12. Our $U_R$ values coincide with the activation energies determined from magnetization studies of Bi2212 superconductors.[71] The lowest activation energies $U_{N2}$ found from the broad Nernst signal spread from 24 to 16 meV. Such a behavior reflects the specific sensitivity of each effect to different pinning mechanisms, as we have pointed out already. The magnetic-field dependence of activation energies fits well the expression

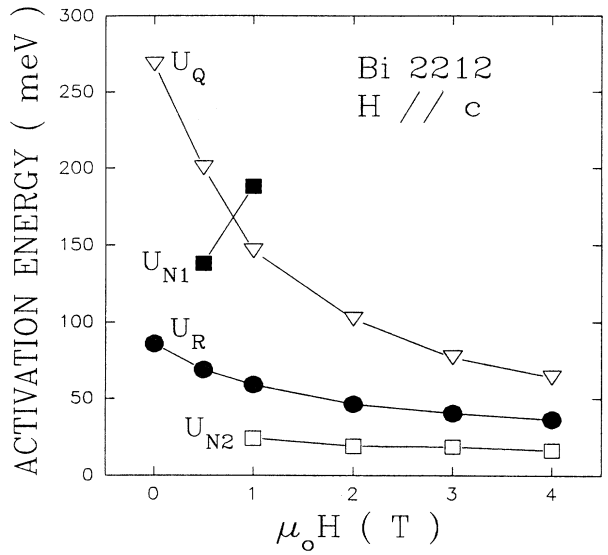


FIG. 12. Activation energy determined from electrical resistance ( $U_R$ ), thermoelectric power ( $U_Q$ ), and Nernst effect ( $U_N$ ).

$$U(B)=U^*\ln(B^*/B) \tag{12}$$

proposed by D'Anna *et al.*,[71] with the exception for the narrow Nernst-effect peak at 88 K marked by $U_{N1}$. The $B^*$ parameters obtained from the fit are 36 and 90 T for resistivity and Nernst effect, respectively. Unfortunately, such an unusual $U_{N1}$ vs $H$ variation cannot be analyzed in detail due to the limited experimental data.

## VI. CONCLUSIONS

In summary, let us point out that we examined various electrical and thermal transport properties of a Bi2212 single crystal in the presence of a magnetic field directed perpendicular to the electrical and temperature gradient. Some emphasis has been put on the excess mixed-state thermoelectric power and on the Nernst effect. The properties have been described and values are in agreement with data for polycrystals. The derived physical properties, such as the excess quantities, vortex transport entropy, Ginzburg-Landau parameter, coherence length, viscous damping coefficient, and thermal Hall angle have been calculated under given assumptions. The range of such quantities was compared to values in similar and related materials being either thin films or polycrystals. The findings point to the need for deeper investigations on the role of vortex density and vortex scattering to describe thermomagnetic transport phenomena.

## ACKNOWLEDGMENTS

Support from NATO HTECH 5-2-05RG/930344, SSTC (Bruxelles) SU/02/13, and ARC 94-99/174 grants are acknowledged. The authors thank Professor H. W. Vanderschueren for allowing us to use the MIEL equipment and Dr. R. Cloots for the scanning electron microscopy analysis. M.P. was supported by Grant BW/95.

*Electronic address: ausloos@gw.unipc.ulg.ac.be
†http://www.phe.ulg.ac.be/

[1]J. R. Clem, in *Physics and Materials Science of High Temperature Superconductors,* edited by R. Kossowski, S. Methfessel, and D. Wohlleben (Kluwer Academic, Dordecht, 1990), p. 79.
[2]A. Dascoulidou, M. Galffy, C. Hohn, N. Knauf, and A. Freimuth, Physica C **201**, 202 (1992).
[3]A. V. Samoilov, A. A. Yurgens, and N. V. Zavaritsky, Phys. Rev. B **46**, 6643 (1992).
[4]N. V. Zavaritsky, A. V. Samoilov, and A. A. Yurgens, JETP Lett. **55**, 127 (1992).
[5]N. V. Zavaritsky, A. V. Samoilov, and A. A. Yurgens, Physica C **180**, 417 (1991).
[6]S.-A. Zhou, Physica C **228**, 122 (1994).
[7]G. Yu. Logvenov, V. A. Larkin, and V. V. Ryazanov, Phys. Rev. B **48**, 16 853 (1993).
[8]H.-C. Ri, R. Gross, F. Gollnik, A. Beck, R. P. Heubener, P. Wagner, and H. Adrian, Phys. Rev. B **50**, 3312 (1994).
[9]M. Pękała and M. Ausloos, Physica C **235-240**, 1385 (1995).
[10]M. Pękała, H. Bougrine, and M. Ausloos, J. Phys. Condens. Matter **7**, 5607 (1995).
[11]M. Pękała, H. Bougrine, T. Łada, A. Morawski, and M. Ausloos, Supercond. Sci. Technol. (to be published).
[12]M. Pękała, R. Cloots, H. Bougrine, E. Maka, and M. Ausloos, Z. Phys. B **67**, 97 (1995).
[13]F. J. Blatt, *Physics of Electronic Conduction in Solids* (McGraw-Hill, New York, 1968).
[14]M. P. A. Fisher, Phys. Rev. Lett. **62**, 1415 (1989).
[15]D. R. Nelson, Phys. Rev. B **39**, 9153 (1989).
[16]M. V. Feigelman and V. M. Vinokur, Phys. Rev. B **41**, 8986 (1990).
[17]E. H. Brandt, Phys. Rev. Lett. **63**, 1106 (1989).
[18]P. Kes, J. Aarts, J. van den Berg, C. J. van der Beek, and J. Mydosh, Supercond. Sci. Technol. **1**, 242 (1989).
[19]M. V. Feigelman, V. B. Geshkenbein, A. I. Larkin, and V. M. Vinokur, Phys. Rev. Lett. **63**, 2303 (1989).
[20]M. G. Blatter, V. B. Geshkenbein, and V. M. Vinokur, Phys. Rev. Lett. **66**, 3297 (1991).
[21]J. H. P. M. Emmen, S. K. J. Lenczowski, J. H. J. Dalderop, and V. A. M. Brabers, J. Cryst. Growth **118**, 477 (1992).
[22]J. C. Soret, L. Ammor, B. Martinie, Ch. Goupil, V. Hardy, J. Provost, A. Ruyter, and Ch. Simon, Physica C **220**, 242 (1994).
[23]K. Kadowaki, Y. Songliu, and K. Kitazawa (unpublished).
[24]M. Brinkmann, H. Somnitz, H. Bach, and K. Westerholt, Physica C **217**, 418 (1993).
[25]I. Van Driessche, S. Cattoir, and S. Hoste, Appl. Supercond. **2**, 101 (1994).
[26]A. B. Kaiser and C. Uher, in *Studies of High Temperature Superconductors,* edited by A. V. Narlikar (Nova Science, New York, 1990), p. 353.
[27]M. Pękała and A. Pajaczkowska, Physica C **156**, 497 (1988).
[28]M. Pękała, K. Kitazawa, A. M. Balbashov, A. Polaczek, I. Tanaka, and H. Kojima, Solid State Commun. **76**, 419 (1990).
[29]M. Pękała, A. Polaczek, and A. Pajaczkowska, in *Progress in High Temperature Superconductivity,* edited by M. Baran, W.

Gorzkowski, and H. Szymczak (World Scientific, Singapore, 1992), p. 264.
[30]M. Pękała, H. Bougrine, M. Ausloos, T. Lada, and A. Morawski, Mol. Phys. Rep. **7**, 249 (1994).
[31]D. V. Livanov and A. V. Sergeev, Phys. Rev. B **48**, 13 137 (1993).
[32]R. Cloots, H. Bougrine, M. Houssa, S. Stassen, L. D'Urzo, A. Rulmont, and M. Ausloos, Physica C **231**, 259 (1994).
[33]S. Sergeenkov, M. Ausloos, H. Bougrine, R. Cloots, and V. V. Gridin, Phys. Rev. B **48**, 16 680 (1993).
[34]S. R. Jha, R. Rajput, D. Kumar, Y. S. Reddy, and R. G. Sharma, Solid State Commun. **81**, 603 (1992).
[35]F. J. Blatt, C. L. Foiles, and D. Greig, *Thermoelectric Power of Metals* (Plenum, New York, 1976).
[36]K. Durczewski and M. Ausloos, Z. Phys. B **85**, 59 (1991); **92**, 409 (1993); Phys. Rev. B **49**, 13 215 (1994).
[37]K. Durczewski and M. Ausloos, Z. Phys. B **94**, 57 (1994).
[38]N. F. Mott and H. Jones, *The Theory of Properties of Metals and Alloys* (Dover, New York, 1958).
[39]J. M. Ziman, *Electrons and Phonons* (Oxford University Press, Oxford, 1962).
[40]K. Durczewski and M. Ausloos, J. Magn. Magn. Mater. **51**, 230 (1985).
[41]M. Ausloos, K. Durczewski, S. K. Patapis, Ch. Laurent, and H. W. Vanderschueren, Solid State Commun. **65**, 365 (1988).
[42]Ch. Laurent, S. K. Patapis, S. M. Green, H. L. Luo, C. Politis, K. Durczewski, and M. Ausloos, Mod. Phys. Lett. **3**, 241 (1989) (compare the schematic Fig. 4 of this work with our Fig. 2).
[43]S. D. Obertelli, J. R. Cooper, and J. L. Tallon, Phys. Rev. B **46**, 14 928 (1992).
[44]L. M. Leon and R. Escudero, Physica B **165-166**, 1211 (1990).
[45]J. A. Clayhold, A. W. Linnen, Jr., F. Chen, and C. W. Chu, Phys. Rev. B **50**, 4252 (1994).
[46]N. V. Zavaritsky, A. V. Samoilov, and A. A. Yurgens, Physica C **185-189**, 1817 (1991).
[47]V. V. Gridin, W. R. Datars, and P. K. Ummat, Solid State Commun. **74**, 187 (1990).
[48]M. Tinkham, Phys. Rev. Lett. **61**, 1658 (1988).
[49]V. Hardy, A. Maignan, Ch. Goupil, J. Provost, Ch. Simon, and C. Martin, Supercond. Sci. Technol. **7**, 126 (1994).
[50]D. Hu, V. A. Brabers, J. H. P. M. Emmen, and W. J. M. de Jonge, Physica C **216**, 315 (1994).
[51]A. Ruyter, Ch. Simon, V. Hardy, M. Hervieu, and A. Maignan, Physica C **225**, 235 (1993).
[52]Yu Fen Guo, P. H. Duvigneaud, H. Bougrine, and M. Ausloos, Physica C **235-240**, 3125 (1995).
[53]Y. Yeshurun and A. P. Malozemoff, Phys. Rev. Lett. **60**, 2202 (1988).
[54]M. P. A. Fisher, Phys. Rev. Lett. **62**, 1415 (1989).
[55]A. Houghton, R. A. Pelcovits, and A. Sudbo, Phys. Rev. B **40**, 6763 (1989).
[56]S. A. Sergeenkov, Solid State Commun. **79**, 863 (1991).
[57]V. V. Gridin, P. Pernambuco-Wise, C. G. Trendall, W. R. Datars, and J. D. Garret, Phys. Rev. B **40**, 8814 (1989).
[58]K. H. Fischer, Physica C **200**, 23 (1992).
[59]F. Kober, R. P. Huebener, H.-C. Ri, A. V. Ustinov, M. Zeh, J. Mannhart, R. Gross, and A. Gupta, Physica B **165&166**, 1217 (1990).
[60]M. Zeh, H.-C. Ri, F. Kober, R. P. Huebener, A. V. Ustinov, J. Mannhart, R. Gross, and A. Gupta, Phys. Rev. Lett. **64**, 3195 (1990).
[61]T. Yoshitake, T. Satoh, Y. Kubo, T. Manako, and H. Igarashi, Jpn. J. Appl. Phys. **27**, L1094 (1988).
[62]Y. Koike, T. T. Nakanomyo, and T. Fukase, Jpn. J. Appl. Phys. **27**, L841 (1988).
[63]R. P. Huebener, *Magnetic Flux Structures in Superconductors* (Springer-Verlag, Berlin, 1979), p. 164.
[64]M. W. Coffey, Phys. Rev. B **48**, 9767 (1993).
[65]O. L. De Longe, and F. A. Otter, Jr., J. Phys. Chem. Solids **33**, 1571 (1972).
[66]R. Job and M. Rosenberg, Physica C **172**, 391 (1991).
[67]M. Kanai, T. Kawai, and S. Kawai, Physica C **185-189**, 1999 (1991).
[68]B. Batlogg, T. T. M. Palstra, L. F. Schneemeyer, R. B. van Dover, and R. J. Cava, Physica C **153-155**, 1062 (1988).
[69]A. Freimuth, in *Superconductivity,* Frontiers in Solid State Science, Vol. 1, edited by L. C. Gupta, and M. S. Multani (World Scientific, Singapore, 1993).
[70]V. Calzona, M. R. Cimberle, C. Ferdeghini, D. Marre, M. Putti, A. S. Siri, R. Flukiger, and G. Grasso, Physica C **235-240**, 3113 (1995).
[71]G. D'Anna, M.-O. Andre, M. V. Indenbom, and W. Benoit, Physica C **230**, 115 (1994).